

#524

RAE-B

RYLE-VONBERG 24-HOUR DATA

73-039A-01B

RAE-B

RYLE-VONBERG 24-HOUR DATA

73-039A-01B

THIS DATA SET HAS BEEN RESTORED. ORIGINALLY IT CONTAINED 11 9-TRACK, 1600 BPI TAPES WRITTEN IN BINARY WITH AN IBM STANDARD LABEL. THERE ARE TWO RESTORED TAPES, THESE TAPES WERE STACKED WITHOUT THE STANDARD LABEL. THE DR TAPES ARE 3480 CARTRIDGES AND THE DS TAPES ARE 9-TRACK, 6250 BPI. THE ORIGINAL TAPES WERE CREATED ON AN IBM 360 COMPUTER AND THEY WERE RESTORED ON THE MRS SYSTEM. THE DR AND DS NUMBERS ALONG WITH THE CORRESPONDING D NUMBERS AND THE TIME SPANS ARE AS FOLLOWS:

DR#	DS#	D#	FILES	TIME SPAN
DR004293	DS004293	D047295	1-15	07/12/73 - 09/09/73
		D047296	16-30	09/10/73 - 11/09/73
		D047297	31-44	11/09/73 - 01/03/74
		D047298	45-59	01/04/74 - 03/04/74
		D047299	60-74	05/04/74 - 07/02/74
		D047300	75-89	07/03/74 - 08/31/74
DR004294	DS004294	D047301	1-15	09/01/74 - 10/30/74
		D047302	16-30	10/31/74 - 12/29/74
		D047303	31-45	12/30/74 - 02/28/75
		D047304	46-60	02/28/75 - 04/29/75
		D047305	61-75	04/29/75 - 06/28/75

REQ. AGENT
GLS

RAND NO.
V0111

ACQ. AGENT
JIV

RAE-B

RYLE-VONBERG 24-HOUR DATA

73-039A-01B

This data set catalog consists of 11 magnetic tapes. Each tape contains 15 files of data, with each file containing 4 days of data. The files are in chronological order. These tapes were created on the 360 computer. These tapes are 1600 BPI, 9-track, IBM standard tapes. The following lists the D numbers, RA numbers, files and the time span for each tape.

<u>D#</u>	<u>RA#</u>	<u>FILES</u>	<u>TIME SPAN</u>
D-47295	RA1370	45	07/12/73 - 09/09/73
D-47296	RA1371	45	09/10/73 - 11/09/73
D-47297	RA1372	42	11/09/73 - 01/01/74
D-47298	RA1373	45	01/04/74 - 03/04/74
D-47299	RA1375	45	05/04/74 - 07/02/74
D-47300	RA1376	45	07/03/74 - 08/31/74
D-47301	RA1377	45	09/01/74 - 10/30/74
D-47302	RA1378	45	10/31/74 - 12/29/74
D-47303	RA1379	45	12/30/74 - 02/28/74
D-47304	RA1380	45	02/28/75 - 04/29/75
D-47305	RA1381	45	04/29/75 - 06/28/75

RAE-2 EXPERIMENT DESCRIPTION

The Radio-Astronomy-Explorer-2 satellite (Explorer-49) was placed in an 1100 km, circular lunar orbit on 15 June 1973. The RAE-2 was instrumented with electric antennas and radio receivers designed to provide sensitive observations of nonthermal radio emissions from the sun, the planets, and the Milky Way at frequencies between 25 kHz and 13 MHz. This document describes the basic data base compiled from the RAE-2 radio receiver experiments. A detailed discussion of the objectives and instrumentation of RAE-2 is given in "Scientific Instrumentation of the Radio-Astronomy-Explorer-2 Satellite" by J.K. Alexander, M.L. Kaiser, J.C. Novaco, F.R. Grena, and R.R. Weber which was published as Goddard Space Flight Center Report X-693-75-40, Feb. 1975 (attachment 1) and which appeared in slightly condensed form under the same title in Astronomy and Astrophysics, vol. 40, pp. 365-371 (1975). Additional information can be obtained in papers listed in the Radio Astronomy Explorer Program Bibliography appended to this document (attachment 2). A list of important RAE-2 operations dates is given in Table 1, and a list of some pertinent experiment parameters is given in Table 2 and shown in Figure 1.

Table 1. Major RAE-2 Event Dates

Launch	10 June 1973
Lunar orbit injection	15 June 1973
Final orbit trim	9 July 1973
V-antenna extension to 183m; experiment turn-on	12 July 1973
First lunar shadow period	29 July-26 Oct. 1973
Upper V-antenna extension to 200 m . .	8 Nov. 1973
Upper V-antenna extension to 229 m . .	14 Nov. 1973
Second lunar shadow period	3 Jan-22 Mar. 1973
Third lunar shadow period	10 June-28 Aug. 1974
One lower V-antenna boom extended to 229 m	11 Oct. 1974
Other lower V-antenna boom extended to 229 m.	6 Nov. 1974
Fourth lunar shadow period	17 Nov. 1974-1 Feb. 1975
Fifth lunar shadow period	21 Apr.-9 Jul. 1975
Begin "new moon intensive" 50% data coverage	1 July 1975
Resume full-time data coverage	24 Dec. 1975
Return to 50% coverage during selected periods	17 Apr. 1976
Resume full-time coverage	19 Oct. 1976

Table 2. Salient RAE-2 Experiment Characteristics

ORBIT

Lunar altitude	1058 x 1070 km
Inclination to lunar equator	59°
Period	222 min

BURST RECEIVERS

Frequency range	0.025-13.1 MHz
Number of channels	32
Sample rate	1 sample / 7.68 sec at each frequency
Bandwidth	20 kHz
Time constant	6 ms
Dynamic range	> 50 dB
Calibration accuracy (relative)	±0.5 dB rms

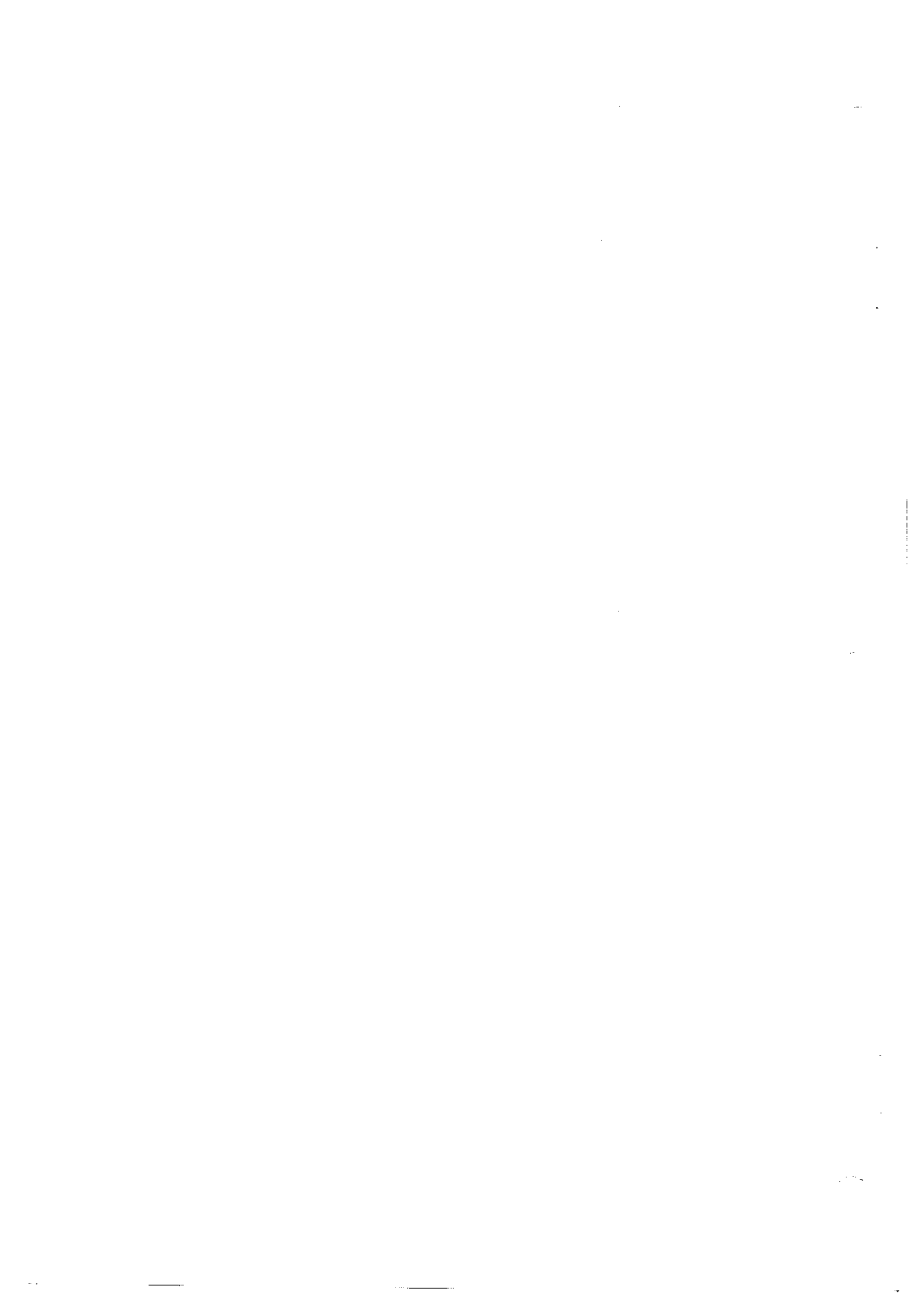
V-ANTENNAS

Full length	229 m
Apex angle	approx. 35°

Table 2 (continued)

RYLE-VONBERG RECEIVERS

Frequency range	0.450 - 9.18 MHz
Number of channels	9
Sample rate	
Coarse	4 samples/7.68 sec at one frequency
Fine	1 sample/7.68 sec at one frequency
Cycle Time	138 seconds
Bandwidth	40 kHz
Time Constant	
Coarse	0.1 sec
Fine	0.5 sec
Dynamic range	60 db
Calibration accuracy (relative)	\pm 3%



Burst Receivers

The RAE-2 burst receivers were 32-channel, stepped-frequency receivers which obtained one sample at each frequency every 7.68 sec. One receiver (BR-1) was connected to the upper V-antenna and one receiver (BR-2) was connected to the lower V-antenna. As shown in the accompanying block diagram (Figure 2) the RF voltage at the feed point of each half of the V-antenna was sampled by a wide-band, high-impedance pre-amplifier, and the pre-amplifier outputs were combined in a balun transformer and fed to the burst receiver. Each burst receiver was comprised of a pair of redundant IF amplifiers and detectors which shared a common set of crystal-controlled local oscillators and mixers. Only one IF strip was powered on at a given time; the other was used as a back-up system. Low-pass filters at the input of the burst receiver prevented strong signals at the 21.4 MHz intermediate frequency from entering the IF strip. Each receiver had a crystal-controlled IF bandwidth of 20 kHz and a post-detection integration time constant of 6 msec. A thermistor located in each burst receiver provided a measurement of the ambient temperature of the receiver, and this information was included in the housekeeping data telemetered every 19.7 min. Also, the normal antenna signal measurement sequence was interrupted for 1.28 min every 19.7 min, and calibration noise source signals were injected into each burst receiver to provide a check of their long term gain stability. The center frequencies for each burst receiver channel are listed in Table 3.

Table 3. RAE-2 Burst Receiver Frequencies

Ch.#	Freq.(kHz)	Ch.#	Freq.(kHz)	Ch.#	Freq.(kHz)	Ch.#	Freq.(kHz)
1	25	9	130	17	475	25	2200
2	35	10	155	18	600	26	2800
3	44	11	185	19	737	27	3930
4	55	12	210	20	870	28	4700
5	67	13	250	21	1030	29	6550
6	83	14	292	22	1270	30	9180
7	96	15	360	23	1450	31	11800
8	110	16	425	24	1850	32	13100

The total dynamic range of the burst receivers was approximately 60 dB and was divided into two 30-dB ranges by logic circuitry in the detector electronics. The least significant bit of each 8-bit telemetry word was used to provide a range flag. The limit of the input signal level resolution due to telemetry quantization step size was about 0.3 dB.

Saturation level signals at the pre-amplifier input often resulted in the generation of intermodulation products in the RF amplifiers which then appeared as wide-band signals in the telemetered data. This problem was most acute when intense kilometer wavelength emissions from the terrestrial magnetosphere were observed at frequencies in the 200-300 kHz range. BR-1 was less susceptible to intermodulation problems than BR-2 by 6 to 10 dB. An example of an event with significant intermodulation interference artifacts is shown in Figure 3.

Due to a failure in the local oscillator circuitry in BR-1, channels 4(55 kHz) and 12 (210 kHz) did not provide useable data.

During periods when a portion of each orbit was in the lunar shadow, cyclic variations in thermal gradients across the V-antenna booms resulted in scissor-mode oscillations of the booms which did not occur when the spacecraft was in 100% sunlight. One consequence of this boom motion was a variation in antenna impedance that sometimes resulted in significant fluctuations in the apparent signal level - especially at frequencies near half- and full-wave resonance (i.e. \sim 737 and 1310 kHz.) This effect had a period of approximately 50 min (the scissor-mode period) and was most pronounced on the upper V-antenna during the first and fifth lunar shadow period (see Table 1) and on the lower V-antenna during the second and third lunar shadow periods.

Daily dynamic spectral plots were generated using BR-2 data in the following fashion. For every 10-minute interval of data, signal intensity distributions, $N(I)$, were calculated at each frequency by sorting the data in 1-dB bins. Then the values of the mean, minimum, and maximum signal levels as well as the mode (most common value) of the distribution were determined for each 10-min interval at each frequency. These data were used to generate four 24-hr dynamic spectral displays which showed the variation of the average, minimum, maximum and mode of the received noise as a function of frequency and time with 10-min resolution. The intensity scale was plotted in increments of 1 dB with respect to the average background level at

each frequency determined from studies of the long-term baseline level. The display format is illustrated and explained in Figures 3 and 4.

The dynamic spectral plots discussed above were generated from data contained on the RAE-2 Burst Receiver Ten Minute Summary Tapes. The contents and format of those tapes are described in Attachment 3.

Ryle-Vonberg Receivers

The RAE-2 Ryle-Vonberg receivers are designed to provide measurements which are relatively insensitive to gain and bandwidth changes. They operate at nine frequencies from 0.45 to 9.18 MHz. There are two receivers - RV-1 connected to the upper V and RV-2 connected to the lower V. The radiometers have an effective bandwidth of 40 kHz and a post-detection time constant of 0.1 second. A coarse output channel is obtained from the integrated servo-loop error signal, and a fine output channel is obtained from the noise source output required to match the antenna signal. (See Figure 5 for a block diagram of the Ryle-Vonberg receivers.) The time constant for the fine channel is 0.5 second. A thermistor located in the receiver measures the ambient temperature which is telemetered every 19.7 minutes in the housekeeping data. The center frequencies for the Ryle-Vonberg receivers are listed in Table 4.

Each frequency is selected for 15.4 seconds before stepping to the next. During this time, eight coarse and two fine samples are taken. Of the eight coarse samples, the first is not reliable since not enough time has elapsed for the receiver to stabilize since the frequency switch was made.

The data from the Ryle-Vonberg receivers are written on a tape containing 15 files with each file representing 4 days of data produced from the 24-hr tapes. The format of the tapes is described in Attachment 4.

Table 4. Ryle-Vonberg Receiver Frequencies

<u>Channel Number</u>	<u>Frequency (MHz)</u>
1	0.45
2	0.70
3	0.90
4	1.31
5	2.20
6	3.93
7	4.70
8	6.55
9	9.18

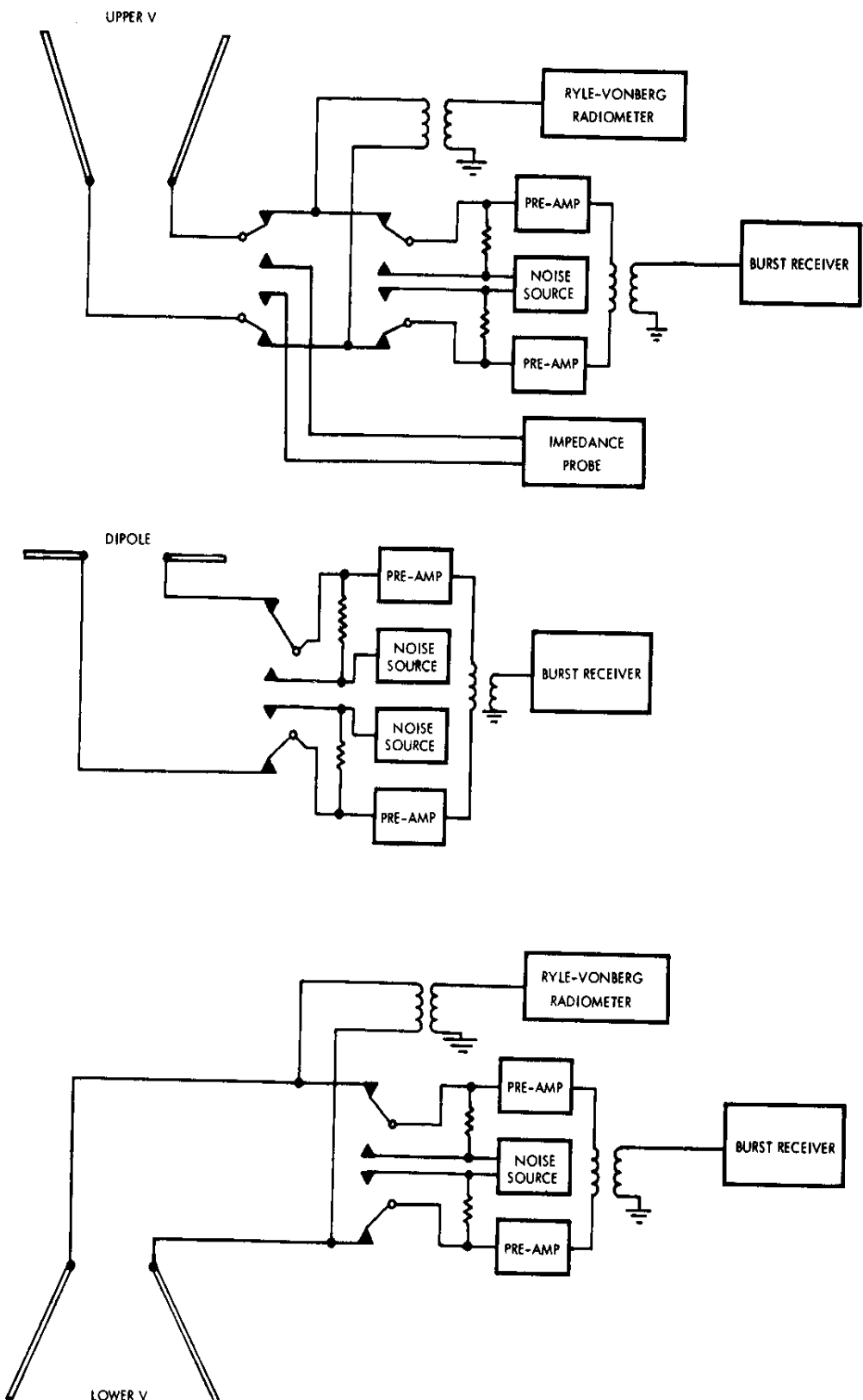


Fig. 1. Block diagram of RAE-2
experiment instrumentation

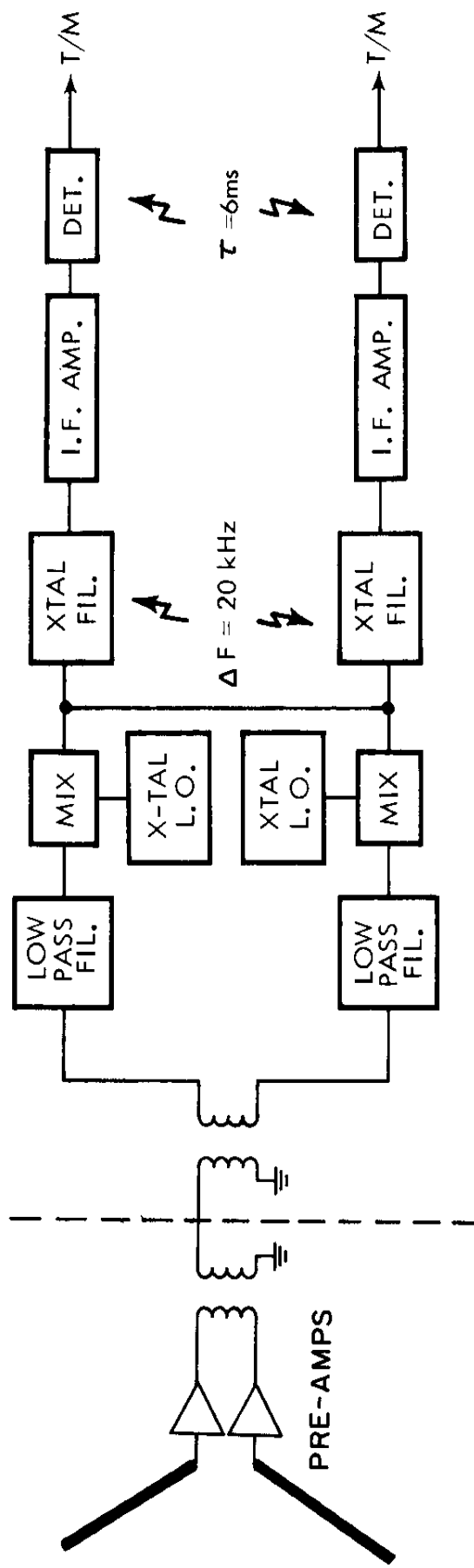


Fig. 2 Block diagram of the RAE-2 V-antenna burst receiver.

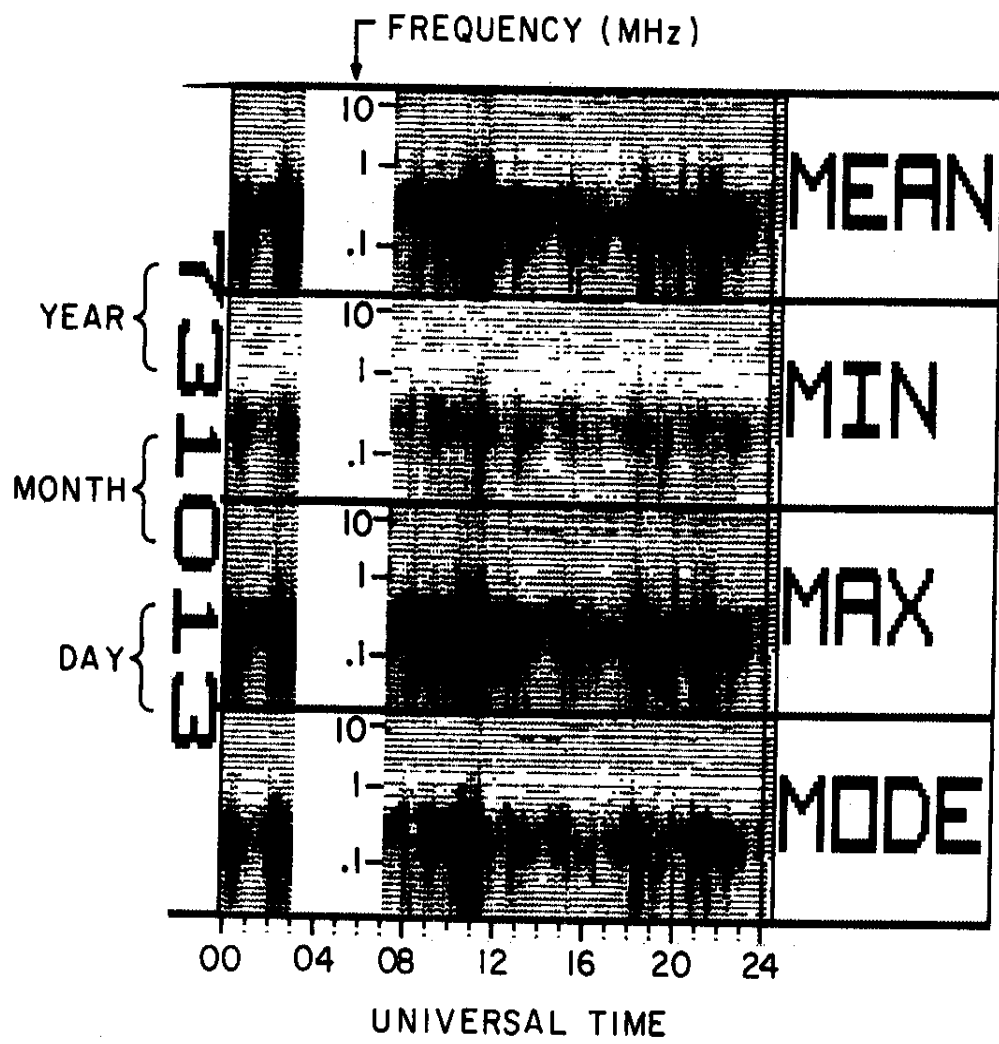


Fig. 3 Twenty-four-hour dynamic spectrum of BR-2 measurements illustrating receiver intermodulation effects due to intense terrestrial noise levels at frequencies near 0.3 MHz. The vertical "stripes" which appear to indicate strong wide-band signal levels (especially near 02-03 hr., 10-12 hr., 18-19 hr., and 21-22 hr. U.T.) are due to intermodulation effects in the pre-amplifiers.

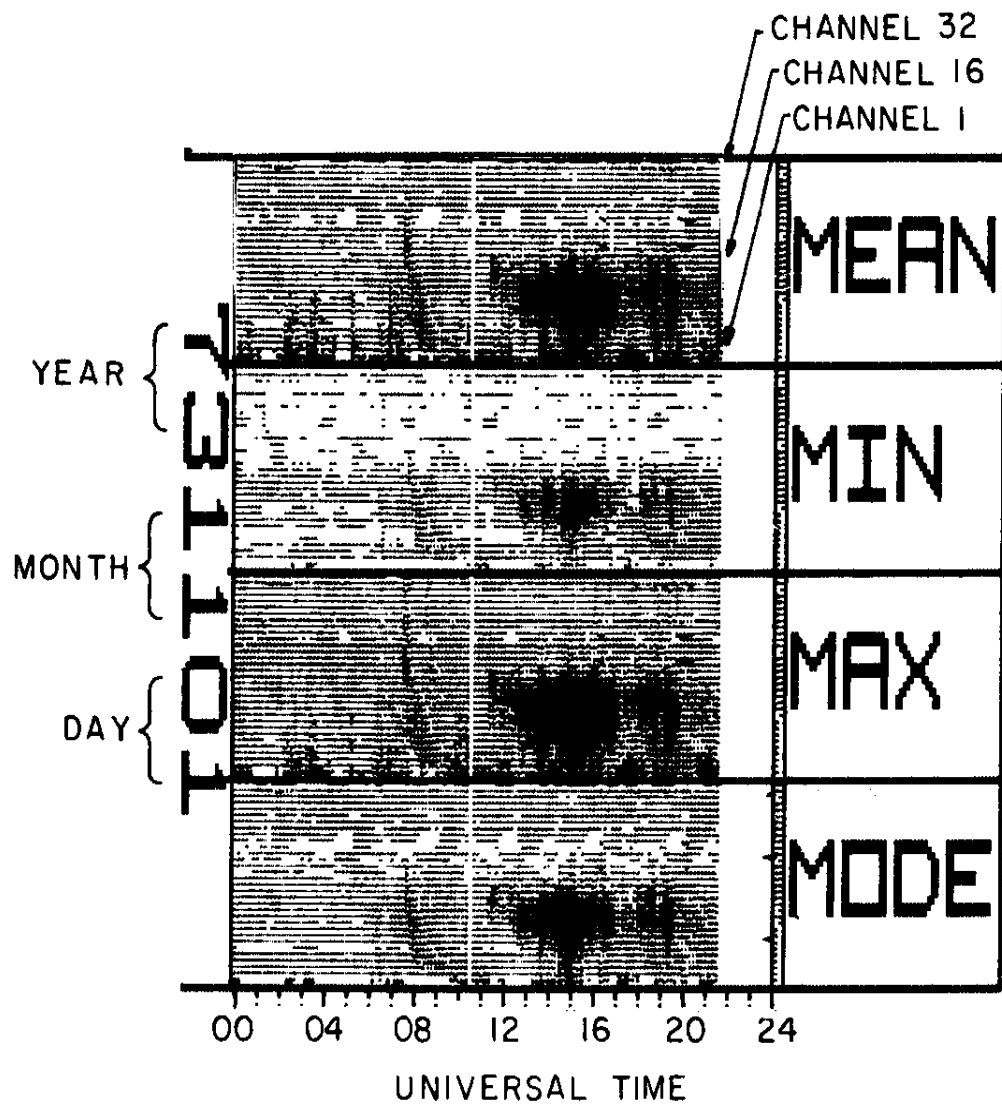


Fig. 4 Example of the 24-hr. dynamic spectral plots generated from the burst receiver ten-minute summary data tapes. Increasing darkness indicates increasing signal intensity. Note (1) some sporadic VLF noise bursts from the solar wind at frequencies below 100 kHz at about 02-04 hr. U.T., (2) a type III solar radio burst at about 08-09 hr. U.T., and (3) a terrestrial kilometer wavelength radio storm at about 13-17 hr. U.T.

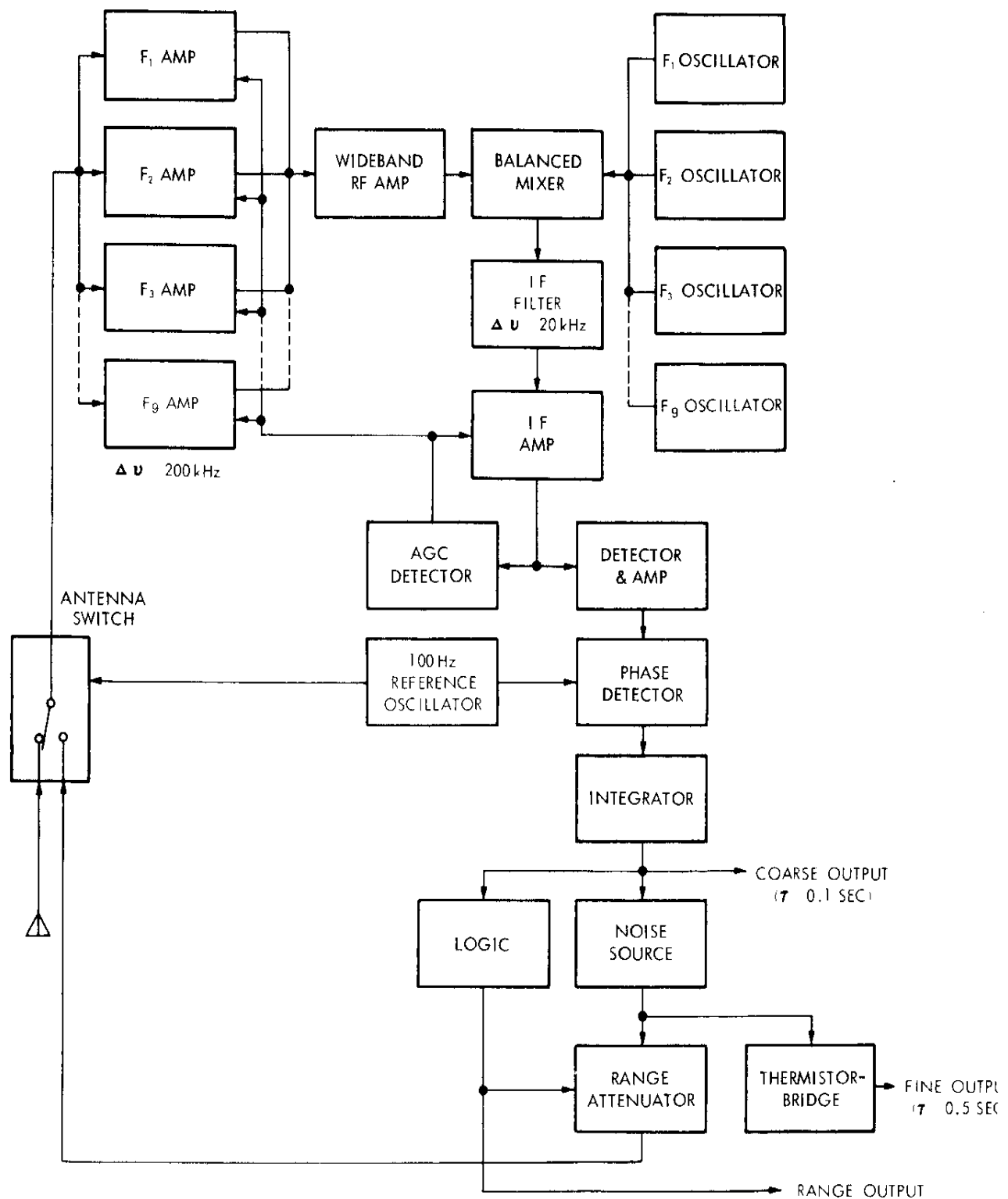


Fig. 5. Block diagram of RAE-2
Ryle-Vonberg receiver

"RADIO ASTRONOMY EXPLORER PROGRAM BIBLIOGRAPHY"

1964

Alexander, J.K. and Stone, R.G. "A Satellite System for Radio
Astronomical Measurements at Low Frequencies", Annales
d'Astrophys., 27, 837.

1966

Flatley, T.W., "Equilibrium Shape of an Array of Long Elastic
Structural Members in Circular Orbit", NASA TN D-3173, March 1966.

1968

Grant, M.M., and Libby, J.N., "Operational Considerations for the
Radio Astronomy Explorer (RAE) Spacecraft", GSFC Document
X-722-68-103, 1968.

Newton, J.K., and Farrell, J.L., "Natural Frequencies of a Flexible
Gravity-Gradient Satellite", J. Spacecraft & Rockets, 5, 560.

1969

Alexander, J.K., Brown, L.W., Clark, T.A., Stone, R.G., and Weber, R.R.,
"The Spectrum of the Cosmic Noise Radio Background Between 0.4
and 6.5 MHz", Astrophys. J., 157, L163, GSFC X-615-69-298, July 1969.

Blanchard, D.L., "Dynamical Performance to Date of RAE-A (Explorer 38)"
GSFC Document X-723-69-214, May, 1969.

Farrell, J.L., and Newton, J.K., "Continuous and Discrete RAE Structural
Models", J. Spacecraft & Rockets, 6, 414.

Farrell, J.L., Newton, J.K., Miller, J.A., and Solomon, E.N., "Optical Estimation of Rotation-Coupled Flexural Oscillations", J. Spacecraft & Rockets, 6, 1290.

Fedor, J.V., Ward, B.W. "RAE Antenna-Damper Package Deployment Interaction", GSFC Document No. X-723-69-251, July 1969.

1970

Alexander, J.K., "New Results and Techniques in Space Radio Astronomy", New Techniques in Space Astronomy, F. Labuhn and R. Lüst eds., 401, D. Reidel Pub. Co. (Dordrecht-Holland, 1971); GSFC Document X-693-70-267, July 1970.

Alexander, J.K., Brown, L.W., Clark, T.A., and Stone, R.G., "Low Frequency Cosmic Noise Observations of the Constitution of the Local System", Astron. and Astrophys. 6, 476; GSFC Document X-615-70-22, Jan. 1970.

Bowers, E.J., and Williams, C.E., "Optimization of RAE Satellite Boom Deployment Timing", J. Spacecraft & Rockets, 6, 1057.

Clark, T.A., Brown, L.W., and Alexander, J.K., "Spectrum of the Extra-Galactic Background Radiation at Low Radio Frequencies", Nature, 228, 847.

Fainberg, J., and Stone, R.G., "Type III Radio Burst Storms Observed at Low Frequencies: Part-I, Storm Morphology", Sol. Phys., 15, 222; GSFC Document X-615-70-186, 1970.

Fainberg, J., and Stone, R.G., "Type III Solar Bursts Storms Observed at Low Frequencies: Part-II, Average Exciter Speed", Sol. Phys., 15, 433; GSFC Document X-693-70-209, 1970.

Kaiser, M.L., "Radio Astronomy Explorer-1 Data Displays", GSFC Document X-693-70-326, 1970.

Mattingly, R.D., Angulo, E.D., Calabrese, M.A., Tyler, A.L., Tumulty, W.T., Sours, W.P., and Burdick, H.F., "Mechanical Design of Radio Astronomy Explorer (A)", GSFC Document X-723-70-255, 1970.

Weber, R.R., "Search for Jovian Hectometric Continuum Radiation", Nature 227, 591.

1971

Alexander, J.K., Brandt, J.C., Maran, S.P., and Stecher, T.P., "The Gum Nebula: Further Evidence from Spacecraft and Ground-based Instruments", Astrophys. J., 167, 487.

Evans, L., Fainberg, J., and Stone, R.G., "A Comparison of Type III Solar Radio Burst Theories Using Satellite Radio Observations and Particle Measurements", Sol. Phys., 21, 198.

Fainberg, J., and Stone, R.G., "Type III Solar Radio Burst Storms Observed at Low Frequencies: Part-III, Streamer Density, Inhomogeneities, and Solar Wind Speed", Sol. Phys. 17, 392; GSFC Document X-693-70-389, 1970.

Fainberg, J., and Stone, R.G., "Hectometric Solar Noise Storms: Detection of Continuum", Astrophys. J., 164, L123.

Sakurai, K., "The Characteristics of the Solar Activity Regions Responsible for the Generation of Type III Radio Bursts at Hectometric Frequencies in Aug 68", Sol. Phys., 16, 125.

Stone, R.G., and Fainberg, J., "A U-type Solar Radio Burst Originating in the Outer Corona", Sol. Phys., 20, 106.

Weber, R.R., Alexander, J.K., and Stone, R.G., "The Radio Astronomy Explorer Satellite, A Low-Frequency Observatory", Radio Sci., 6, 1085.

1972

Novaco, J.C., Vandenberg, N.R., "A Model of the Local Region of the Galaxy", GSFC Document X-693-72-8, 1972.

Sakurai, K., "Solar Energetic Particles and Wide-Band Continuum Storms from Metric to Hectometric Frequencies", Planet. Space Sci., 21, 17.

Weber, R.R., "A Revised Low-Frequency Cosmic Noise Spectrum", Astron. J., 77, 707.

1973

Evans, L., Fainberg, J., and Stone, R.G., "Characteristics of Type III Exciters Derived from Low Frequency Radio Observations" Sol. Phys., 31, 501.

Fainberg, J., and Stone, R.G., "Satellite Observations of Type III Solar Radio Bursts at Low Frequencies", Space Sci. Rev., 16, 145; GSFC Document X-693-73-346, 1973.

Grant, M.M., and Comberiate, M.A., "Operating the Radio Astronomy Explorer-B Spacecraft (RAE-B)", GSFC Document X-714-72-97, 1973.

Herman, J.R., Caruso, J., and Stone, R.G., "Radio Astronomy Explorer (RAE-1) Observations of Terrestrial Radio Noise", Planet. Space Sci., 21, 443.

Howard, E.G., "A Storm of Type III Bursts Observed by RAE-1 in August 1968", High Energy Phenomena on the Sun, ed. by R. Ramaty and R. Stone, 552, NASA SP-342.

Novaco, J.C., "Galactic Background Maps at 3.93 and 6.55 MHz", GSFC Document X-693-73-182, 1973.

Stockwell, J.M., "Data Processing Plan for Radio Astronomy Explorer Satellite-B Lunar Mission", GSFC Document X-565-73-300, 1973.

Stone, R.G., and Fainberg, J., "Solar Radio Bursts at Kilometer Wavelengths" High Energy Phenomena on the Sun, ed. by R. Ramaty and R. Stone, 519, NASA SP-342.

Stone, R.G., "Radio Physics of the Outer Solar System", Space Sci. Rev., 14, 534.

1974

Alexander, J.K., and Clark, T.A., "Radio Astronomy", High Energy Particles and Quanta in Astrophysics, F.B. McDonald and C.E. Fichtel eds., 274, MIT Press (Cambridge, Mass. 1974).

Alexander, J.K., and Novaco, J.C., "A Survey of the Galactic Background Radiation at 3.93 and 6.55 MHz", Astron. J., 79, 777; GSFC Document X-693-73-63, Mar. 1974.

Bryant, W.C., and Williamson, R.G. "Lunar Gravity Analysis Results from Explorer 49", Amer. Inst. Aeronautics and Astronautics paper No. 74-810, Aug. 1974.

Desch, M.D. and Carr, T.D., "Dekametric and Hectometric Observations of Jupiter from the RAE-1 Satellite", Astrophys. J. (Lett.) 194, L57.

Fainberg, J., "Solar Radio Bursts at Low Frequencies", Coronal Disturbances ed. by G. Newkirk, D. Reidel Pub. Co. (Dordrecht-Holland, 1974).

Fainberg, J. and Stone, R.G., "Satellite Observations of Type III Solar Radio Bursts at Low Frequencies", Space Sci. Rev., 16, 145.

Mosier, S.R., and Kaiser, M.L., "Calibration of a Cylindrical RF Capacitance Probe", J. Geophys. Res. 80, 702; GSFC Document X-693-74-205, July 1974.

Lawlor, E.A., Davis, R.M., and Blanchard, D.L., "Engineering Parameter Determination from the Radio Astronomy Explorer (RAE-1) Satellite Attitude Data", Amer. Inst. Aeronautics and Astronautics paper No. 74-789, Aug. 1974.

Sakurai, K., "Solar Longitude Dependence of some Characteristics of Type III Radio Bursts from Metric to Hectometric Wavelengths", Sol. Phys., 36, 171.

Sakurai, K., "Solar Radio Continuum Storms", GSFC Document X-693-74-331, Nov. 1974.

Stone, R.G., "Travelling Solar Radio Bursts", Solar Wind Three ed. by C.T. Russell, 72 (UCLA, 1974).

1975

- Alexander, J.K., Kaiser, M.L., Novaco, J.C., Grena, F.R., and Weber, R.R., "Scientific Instrumentation of the Radio-Astronomy-Explorer-2 Satellite", Astron. Astrophys., 40, 365; GSFC X-Document 693-75-40, Feb. 1975.
- Herman, J.R., Stone, R.G., and Caruso, J.A., "Radio Detection of Thunder-storm Activity with an Earth-Orbiting Satellite", J. Geophys. Res., 80, 665.
- Kaiser, M.L. and Stone, R.G., "Earth as an Intense Planetary Radio Source: Similarities to Jupiter and Saturn", Science, 189, 285.

1976

- Alexander, J.K., "New Vistas in Planetary Radio Astronomy", Sky & Telescope, March 1976.
- Alexander, J.K. and Kaiser, M.L., "Terrestrial Kilometric Radiation: 1-Spatial Structure Studies", J. Geophys. Res., 81, 5948.
- Kaiser, M.L. and Alexander, J.K., "Source Location Measurements of Terrestrial Kilometric Radiation Obtained from Lunar Orbit", Geophys. Res. Lett., 3, 37.
- Mosier, S.R., "Observations of Magnetospheric Ionization Enhancements Using Upper Hybrid Resonance Noise Band Data from the RAE-1 Satellite", J. Geophys. Res., 81, 253.
- Weber, R.R., Fainberg, J., and Stone, R.G., "Low-Frequency Radio Observation of the Solar Wind", Geophys. Res. Lett., 3, 297.

1977

Alexander, J.K. and Kaiser, M.L., "Terrestrial Kilometric Radiation:
2 - Emission from the Magnetospheric Cusp and Dayside Magneto-
sheath", J. Geophys. Res., 82, 98.

Fitzenreiter, R.J., Fainberg, J., Weber, R.R., Alvarez, H., Haddock, F.T.,
and Potter, W.H., "Out-of-Ecliptic Trajectories of Low Frequency
Type III Bursts", Sol. Phys., in press.

Kaiser, M.K., "A Low Frequency Radio Survey of the Planets with RAE-2",
J. Geophys. Res., 82, 1256.

Kaiser, M.L. and Alexander, J.K., "Terrestrial Kilometric Radiation:
3 - Average Spectral Properties", J. Geophys. Res., in press.

8

ATTACHMENT 3

TAPE FORMAT FOR THE RAE-2 BURST RECEIVER TEN MINUTE SUMMARY TAPES

EACH LOGICAL RECORD CONTAINS A SUMMARY OF TEN MINUTES OF DATA FROM THE BR-1 AND 2 RECEIVERS. THE TEN MINUTE INTERVALS ARE DEFINED TO START AT PRECISELY 0 HR ON EACH DAY. THE LOGICAL RECORD LENGTH IS 544 8-BIT BYTES + A 4 BYTE LOGICAL RECORD CONTROL WORD. THE PHYSICAL RECORDS ARE 32336 BYTES ($=548 \times 59 + 4$). THE TAPES ARE 9-TRACK 1600 BPI. EACH TAPE CONTAINS TWO CALENDAR YEARS OF DATA. THE INDIVIDUAL QUANTITIES IN EACH RECORD ARE

FORTRAN WORD #	TYPE	LENGTH	DESCRIPTION
		BYTES	
1	I	4	DATE IN YYMMDD FORM (E.G. MAY 15, 1974=740515)
2	I	4	UT IN ELAPSED SECONDS FROM 0HR AT THE START OF TEN MINUTE INTERVAL
3,4,5	R	4	LUNICENTERED X,Y,Z OF SPACECRAFT IN KM AT THE ABOVE TIME. THE X AXIS POINTS TOWARD 1ST POINT OF ARIES AND Z IS PARALLEL TO THE EARTH'S SPIN AXIS--THE SYSTEM IS PARALLEL TO GEOCENTRIC EQUATORIAL SYSTEM BUT TRANSPOSED TO THE MOON.
6,7,8	R	4	LUNICENTERED X,Y,Z OF THE EARTH IN UNIT VECTOR FORM AT THE ABOVE TIME

THE FOLLOWING SET OF 8 BYTES IS REPEATED FOR EACH FREQUENCY (IN THE SAME ORDER AS TABLE 3) FOR BOTH RECEIVERS ($8 \times 32 \times 2 = 512$ BYTES = WORD NOS. 9-136). THE 2% VALUES AND THE MODES WERE DETERMINED BY FORMING HISTOGRAMS (FOR EACH FREQUENCY AND RECEIVER) IN 1 DB INCREMENTS FROM THE INDIVIDUAL SAMPLES TAKEN DURING THE 10 MINUTE INTERVAL. THE HISTOGRAMS WERE THEN SCANNED TO FIND THE LOWEST BIN CONTAINING AT LEAST 2% OF THE TOTAL NUMBER OF SAMPLES, THE HIGHEST BIN CONTAINING 2% OF THE TOTAL, AND THE BIN CONTAINING THE MOST SAMPLES (MODE). IN SOME CASES, NO BIN CONTAINED AT LEAST 2% OF THE VALUES, SO A ZERO WAS WRITTEN ON THE TAPE.

TYPE	LENGTH	DESCRIPTION
	BYTES	
I	1	NUMBER OF NON-ZERO SAMPLES DURING THIS TEN MINUTE INTERVAL FOR THIS FREQUENCY AND RCVR
I	1	2% MINIMUM IN DB ABOVE 1 DEGREE KELVIN
I	1	2% MAXIMUM IN DB ABOVE 1 DEGREE KELVIN
I	1	MODE (MOST COMMONLY OCCURRING VALUE) IN DB ABOVE 1 DEGREE KELVIN
I	2	$100 \cdot \text{ALOG10}(\sum T_i)$ WHERE T_i IS A SAMPLE
I	2	$100 \cdot \text{ALOG10}(\sum T_i^2)$

THIS TAPE COULD BE READ AS FOLLOWS (IN IBM 360 FORTRAN IV):

```
LOGICAL*1 NUM(32,2),MIN(32,2),MAX(32,2),MODE(32,2)
INTEGER*2 SUMT(32,2),SUMTSQ(32,2)
READ(IUNIT) IYMD,ISEC,XM,YM,ZM,XE,YE,ZE,
```

```
1 ((NUM(I,J),MIN(I,J),MAX(I,J),MODE(I,J),SUMT(I,J),SUMTSQ(I,J),
2 I=1,32),J=1,2)
```

HOWEVER, A CHEAPER (IN CPU \$) METHOD USING EQUIVALENCE IS:

```
INTEGER*4 A(136)
INTEGER*2 SUMT(4,32,2),SUMTSQ(4,32,2)
LOGICAL*1 NMMM(8,32,2)
EQUIVALENCE (A(1),IYMD),(A(2),ISEC),(A(3),XM),(A(4),YM),
1 (A(5),ZM),(A(6),XE),(A(7),YE),(A(8),ZE),
2 (A(9),NMMM(1),SUMT(1),SUMTSQ(1))
READ(IUNIT) A
```

FOR NMMM USE ONLY ROWS 1,2,3,4 FOR NUM,MIN,MAX,MODE

FOR SUMT USE ONLY ROW 3

FOR SUMTSQ USE ONLY ROW 4

%

7 RA 1370 -

RA 1381

ATTACHMENT 4

Tape Format for the RAE-2 Ryle-Vonberg 24-Hr tapes

Each tape contains 15 files of data, with each file containing 4 days of
 data. The files are in chronological order. The tapes are ~~1600~~⁶²⁵⁰ BPI,
 9-track, ~~IBM standard label tapes~~. The logical record length is 908 bytes,
 consisting of a 4 byte logical record control word and 904 data bytes.
 The physical record length is 31784 bytes long, consisting of a control
 word and 35 logical records.

Each logical record is formulated as follows:

Word #	Tape	Length (Bytes)	Description
0	I	4	logical record control word (to be ignored)
1	I	4	Date, YYMMDD
2	I	4	Milliseconds of day
3	I	4	Frequency where 9 = 9.18 MHz and 1 = 0.45 MHz, etc.
4,5,6	R	4	X, Y, z of spacecraft in km. X-axis points toward the vernal equinox, the z axis is parallel to the earth's spin axis
6,7,8	R	4	X, Y, z of earth's unit vector in luniscentered form
10, 11	R	4	Right ascension and declination (1950.0) of the upper V.
12-18	R	4	Seven RV-1 coarse samples
19-20	R	4	Two RV-1 fine samples
21-27	R	4	Seven RV-2 coarse samples
28-29	R	4	Two RV-2 fine samples
30-225			Repeat of words 2-29 eight times for the remaining sets of this frequency in this sequence
226	I	4	RV ambient temperature

In IBM 360 Fortran IV, the tape could be read as follows:

```
REAL*4    A(226), RV(28,8)  
INTEGER *4    IRV(28, 8)  
EQUIVALENCE  (A(1), IYMD), (A(2), RV(1,1), IRV(1,1))  
READ (IUNIT) A
```

DRDSD4393

FILE 1	REC 340 1	31784 BYTES - 13012
(0)	7C21E2A00	038C0000
(1)	405403F1	41623AA2
(F0)	02A81440	00000000
(120)	00000000	00000000
(160)	C22179E3	00000000
(240)	02201440	00000000
(240)	00000005	C332415E
(240)	45312C35	45BDAC2
(320)	02010300	00000000
(360)	439456EA	C36036A7
(400)	45B3E4B3	45B9E4B3
(440)	02000000	00000000
(480)	40212675	405DF31
(520)	46112F75	4611AB3B
(560)	46473D75	4642DD76
(600)	400EAB652	4178C257
(640)	4E12F115	461596EB
(680)	46317615D	4629DFBE
(720)	C2139420	4611EA4C8
(760)	46113765	4618C0B0
(800)	02000006	C366EC45
(840)	45A1A922	45AB4022
(880)	4F1157B9	46120B05
(920)	02010303	00000005
(960)	02010303	00000000
(1000)	02010300	00000000
(1040)	C324B457	438663C7
(1080)	02010300	00000000
(1120)	02010300	00000000
(1160)	C3515CDF	40244F50
(1200)	46211931	46224AB38
(1240)	02010300	00000000
(1280)	47E15BFD	465AB52
(1320)	46223A2	46239C95
(1360)	02010300	00000000
(1400)	41754B63	C210D755
(1440)	4E21149F	4635D054
(1480)	04541PFC9	00000005
(1520)	4521PTE54	462276E5
(1560)	46472B08	4638C752
(1600)	C355E977	43797E32
(1640)	46212E54	46276E5
(1680)	465RAFCE	465883A2
(1720)	C34F5A12	4023E491
(1760)	46212F94	462CA9C4
(1800)	45414AFCE	463BC75A
(1840)	43012F00	00000000
(1880)	02010300	00000000
(1920)	02010300	00000000
(1960)	46212F24	405ED529
(2000)	4E1127D3	46125E21
(2040)	02010300	00000000
(2080)	465A57CA	416CB043
(2120)	46112C24	4613DC24
(2160)	02010300	00000000
(2200)	4609063DF	4611C93D
(2240)	C211921F	00000000

INDEX DRAFT OF AL 1993

DUMP OF TAPE RA1381

INPUT TAPE RA1381 ON UNIT 4
DATA INPUT H9 NF 45 SK 2 1 1 SK 2 LAST 1 SK 44 1 1 SR 44 LAST 1

D-47385
04/29/75-06/28/75

FILE		INPUT RECS.	DATA RECORDS MAX.	SIZE	PERM	READ ERROR SUMMARY	INPUT RETRIES
FILE	RECORD	1	LENGTH	31	BYTES	0	0
1	3	3	75/04/29	80	0	0	0
(3)	7020000	030000000	000000000	000000000	435C3CBB	437C9205 C350A35A 40140679 406DB4C
(40)	405C8418	412F2134	C21F4C09	456B3337	45705DF4	45705DF4 456862A0 4581E898 456862A0
(80)	456A0019	4570F6C9	46102471	46134105	459BD8B	461961BD 46134105 46113B72
(120)	45D67857	028D3D09	000000008	435B7968	4382A081	4013EEA5 40EDDBB 405C82FA 41312452
(160)	C21B7D20	4581E892	4581E898	458B3337	458R3337	4578F594 459FD2D0 4577D9A6 457D7F9B
(200)	46161B4C	46161B4C	46161C502	462175B3	46161B4C	462175B3 46121EBD 028F5902
(240)	00000008	435A53E4	43383B13	C33D0233	4013D600	40ED028 405C81DB 4133D2B4 C2188991 456862A0
(280)	457C5F94	45705DF4	458B3337	4581E898	45705DF4	458B3337 4570B689 457E4B8 461961BD 4610C502
(320)	46161B4C	46161B4C	461961BD	46161B4C	46266ACB	4610AA24 4610DA0 029174FC 0000008 4358CA0A
(360)	4380315	C332C792	4013BEFB	40EDE294	405C8084	4134C176 C2151A92 45705DF4 456862A0 45705DF4
(400)	4576F594	45705DF4	456862A0	458613C88	458613C88	46134105 46134105 46134105 46161B4C
(440)	4610D2471	46134105	46134105	46113B72	45ED23E5	00000005 029390F5 0356DC73 C32853F1
(480)	4013A726	40ED4FD	405C7F9B	41366572	C211A3E6	455FA3CF 4581E898 456862A0 456862A0
(520)	45705DF4	456662A0	456A0019	45705E89	4569B088	4610C502 459E9B08B 46134105 461961BD 4610C502
(560)	4910C502	45E18560	461363DB	0295ACEE	00000008	4354906E 439543ED C31D8487 40138F53 40EDE764
(600)	495C773F	4137F3E4	C1E126CB4	45662A0	45605F4	455FA3CF 456862A0 456862A0
(640)	455A93BF	455E842A	46161B4C	46102471	46161B4C	46161B4C 46161B4C 46161B4C
(680)	4610A24	0297C8L3	00000008	4351E784	43985A55	C312F451 4013777E 40EDE9C9 406C7D57 4139705C
(720)	C1AA4038	45E1E9C	45705DF4	461F968C	4581E898	45B239E3 459FD2D0 458B3337 461CA5B6 45BE3970
(760)	4540F9FB	452A4950	00000000	46161B4C	463A25AC	453D6F97 00000000 462F0DC69 461E73B7 0299E4E1
(800)	00000008	439AC1B6	C281E56F	40135F5A	40EDEC2D	405C734 413ADD95 C171C286 458B3337
(840)	46116938	45CE7B5	459527B5	45CD7B5	47216CFA	40000000 46155E48 458AE86C 46161B4C 4548AE65
(880)	4535E83A	46E5AEC8	44221E56	46580263	4818E7F9	46104F79 455576C9 411CCCCC 000B735D C21EECB
(920)	02885D0F	0000007	435C2B56	43704653	C34F93FD	401403D3 40EDDB91 405C83F8 412F5C7D 4139705C
(960)	457586E8	455ECE6	455B6486	45671240	457586EB	455B6486 45581FBC 454FC265 45496244 454F0076
(1000)	4549C583	454F0076	454F0076	45575344	454F0076	4544E313 4548C485 028D7908 00000007
(1040)	43505E98	4353537D	C345E1CA	4013E56F	400DDE00	405C82DA 41315B68 C2188F96 455B6486 455EC86C
(1080)	457586E8	455ECE6	45506486	455B6486	454E8C6	45596ECB 4544E313 454F0076 45608656
(1120)	454F0076	45575344	454F0076	45575344	4546283D	454E48A4 028F9502 00000007 435A2DC7 438800F7
(1160)	C33BE2E0	4013D42A	40EDE06D	405C818B	4133360A	C218285F 45581FBC 455EC86C 45581FBC 45581FBC
(1200)	455EC86C	45671240	454F0076	45575344	454F0076	4544E313 4548C485 028D7908 00000007
(1240)	45575344	4544E313	45483E85	4544E313	0291B083	40000007 45158F63 4380B396 C331A03C 4013BC55
(1280)	40EDE2D2	405C809B	4134A10E	C214B353	455F1FBC	455F0076 45596ECB 4544E313 454F0076 45581FBC
(1320)	45586436	45514BAF	454C6B1E	4549C588	4549C588	4549C588 4549C588 4549C588 454F0076 4544E313
(1360)	4544E313	454623D	0293CCF4	00000007	4356A001	4391FC63 C32727B 4013A481 40EDE542 405C7F7B
(1400)	413692C3	C21140FC	456B6486	45671240	45671240	455EC86C 457586EB 455B6486 455EC04B6
(1440)	45578E0E	4549E4588	4549C588	4554F0076	4557334	4544F0076 4544E313 4548C485 4549C588 4543A3E2
(1480)	0295E8E0	00000037	43544E313	43954E313	4549E4588	4549E4588 4549E588 454136B1 4543A3E2
(1520)	45901753	455EC86C	458369AE	45AD3C47	45671240	457586EB 457369AE 45702547 45608656 4544F0076
(1560)	454F0076	45575344	4544E313	4549C588	454F0076	4543A3E2 0298047 00000007
(1600)	4351948D	4398A4AC	C311C0A0	401374D8	40EDEAUE	405C7D37 4139996 4139996 455EC86C 45581FBC
(1640)	45671240	455EC86C	45671240	455E8C6	455B6486	45520DC8B 4557BEE 4544E313 4549C588
(1680)	4544E313	45575344	4544E313	4549A667	4510E4A3	40138ECA0 40EDE7A9 405C7D57 4139705C
(1720)	C26E95A3	40135D05	40EDECT0	405C7C14	41360564	41687743 457586EB 45671240 455B6486 45671240
(1760)	45671240	45671240	45573E0E	455827C8	45378069	4544E313 4549E588 4549E588 454F0076
(1800)	4549C588	4549C588	4544E313	4549A3E2	411CCCCC	038C0000 000B735D 028B990E 00000006 435C19F0
(1840)	437NF2E1	C34E84A0	4014012E	40EDDB0D6	405C83D8	412F9724 C21E80CC 45885866 45885866 45885866
(1880)	45865666	45865666	4592C544	45855866	458012B6	45771343 45787E1B 45771343 45771343 45771343
(1920)	45771343	4577E71R	45787E71R	4598F371	45A35C53	028D508 435B8309 4383F8DE C344CA1C
(1960)	4013E959	40EDDE46	405C82B8A	4131E258	C21H2F66	45885866 45771343 45771343 45771343 45771343
(2000)	45772B5	45772B5	45E94E8	45771343	45771343	457B7E1B 457B7E1B 457B7E1B 457B7E1B 457B7E1B
(2040)	45787E1B	45A33C53	45A33C53	02FD101	00000006 435A0430 43896186 C33AC13F 4013D184 40EDE0B2	
(2080)	405C19E	413364C	C217C6E2	459UFE47	45885866 45885866 45885866 45885866 45885866	
(2120)	455FEE94	45DC6C42	457H7E1B	45771343	45771343 45771343 45771343 45771343 45771343	

(30050)	461032EF	4611763	0050E90B	000J0009	C3632212	C39131FC	42D3CD28	C01C4015	40EE7F89	4058A315
(30120)	41FF7620	41C72589	45FB4049	45DF6B7D	4613DBF7	4613DBF7	45FB4048	45FB4048	4611A8CF	45D3700F
(30160)	45C6D0DA	468047F9	45613B33	00000000	461CB5EF	46FEFA47	455911C7	455911C7	472ECF9A	486C5673
(30220)	005FA409	00000009	C36JDC71	C3937640	4225AD92	C01C5777	40EE7DC1	4058A06A	42100839	418E8F02
(30240)	46165548	4613DBF7	46165548	4613DBF7	4623B812	4613DBF7	46165548	46181C70	46285ED4	4610323C
(30260)	45948C51	456B6UBC	45E04224	45DD14A0	45C93EE98	46133CDA	46183BC6	0061C008	0000009	0000009
(30320)	C3573168	C3952022	C2889988	C01C6ED0	40589RDC0	4210191B	41561E42	4613DBF7	45DF6B7D	45D3700F
(30360)	4613DBF7	45F84048	45DE6B7D	45E666772	45E666772	45E666772	45E666772	46127C4E	4613DBF7	45DF6B7D
(30400)	4A195F4F	464541EA	45385ABB	458013C6	465B2D8B	46133CDA	0063DC07	00000009	C35B229A	C3962C19
(30440)	C313652D0	C01C6639	40EE7A29	40589B14	42102A29	4110D746	45FB404B	45DF6B7D	4611A8CF	45C6ABA9
(30480)	45D6B7D	4564GABA9	45C6ABA9	45320F70	45AC0BB6	4A1AE0D42	45F8025C	46127C4E	4610ED68	46160B9D
(30520)	4610D68	45E31ADD	45C51591	45E80DA6	0065F806	00000009	C357B0A3	C39694A8	C31E2BA3	C01C9D99
(30560)	40EE785B	40589E68	42103B85	C11A000	457179B7	457179B7	457CC2FF	4588B13F	457179B7	457179B7
(30600)	457179B7	4567EA2F	45660F88	A4312C6C	455F8EC1	4558601D	4585E5C4	4558601D	456752EC	45TA9C8D
(30640)	4562EC53	45647F65	00681404	00000009	C353E38D	C39660A4	C328D296	C01CB4F8	40EE768A	405895BA
(30680)	42104D4D	C1522884	00000000	457CC2FF	4588B13F	457179B7	457CC2FF	4568A646	457179B7	4568BAAT
(30720)	45643D10	4A3023AC	455F8EC1	456752EC	45883975	4591EEB5	45883975	457F0AC0	45839E4E	457C471D
(30760)	006A3003	00000009	C34FBF55	C39590E8	C3334F68	C01CCC58	40EE74F8	455F8EC1	45695F60	456618D4
(30800)	00000000	457179B7	457CC2FF	457179B7	4588B13F	457179B7	45695F60	45695F60	45695F60	45883975
(30840)	456752EC	455F8EC1	455F8EC1	45704697	456752EC	45704697	45647F65	45695F60	45643D10	4A312C6C
(30880)	000B7420	005BAA0C	00000008	C364CDA4	C38EAAF1	4316DDC4	C01C2B4D	40EE811D	4058A572	41FE85A1
(30920)	41F99068	45883975	45883975	45883975	4591EEB5	45883975	45883975	457F0AC0	45839E4E	457C471D
(30960)	45C08C26	45DA7A96	45D08C26	45D08C26	45DA7A96	4589C26	4589C26	4589A2C6	45839E4E	45883975
(31000)	00000008	C362E5AC	C39178C5	42C079E0	C01C42AF	40EE7F56	4058A2C9	41FF941B	41C0DAG6	005DC4OB
(31040)	4570FAC0	4591EEB5	4591EEB5	4591EEB5	4591EEB5	45883975	45821DCA	4580A1CA	4567A976	45C08C26
(31080)	C01C7171	40EE7BC3	40589D74	45DA7A96	45C08C26	45A9B177	45B07D1C	45ADB2A5	005FE009	00000008
(31120)	C393AD4	42124E0D	C01C5A10	40EE7D8E	4058A01E	42100A18	41884778	4592F88	4591EEB5	45883975
(31160)	4591EE05	45883975	4591EEB5	4591EEB5	4589C26	4589C26	4589C26	4589A4A4	45839E4E	45883975
(31200)	45A9B177	45C08C26	45A9B177	45B334E	45C03401	0061FC08	0000000	0000000	457E72E	45958D71
(31240)	C12079B3	45883975	45883975	45883975	4591F0AC8	4592C2F88	4591EEB5	0350E875	0350E875	C29BF357
(31280)	4591EEB5	45ACE62A	45883AB0	4598CC52	4631A39	4559B1D0	45444B31	0000000	461194A4	4621112E
(31320)	456B91D8	45C85599	463D782C	00641807	00000008	C35AC415	C3963D92	C31498A3	C01C88D2	40EE79F6
(31360)	40589AC8	42102C14	417179E7	4591EEB5	4591EEB5	4591EEB5	45883975	45883975	45883975	45883975
(31400)	457B110F	457F29E8	45A9B177	45A9B177	45D07A96	45D07A96	4613DBF7	45958D71	45AAF37A	45AAF37A
(31440)	4598E684	00663406	00000008	C3574906	C39696C0	C31F5C6F	C01CA032	40EE7827	4058981C	42103D79
(31480)	C12079B3	45883975	457F0AC0	4591EEB5	457F0AC0	45883975	457F0AC0	45883975	4580A1CA	4585235B
(31520)	45A9B177	45283CD20	45767190	45A9B177	45767190	45C08C26	45958D71	457AB067	45869807	00685004
(31560)	00000008	C355732E	C3965361	45883975	C329FFC7	C01CB791	40EE7656	4058956E	42104F4D	C1585C45
(31600)	457F0AC0	45763F8D	457F0AC0	45883975	45883975	45883975	45883975	45821DCA	457471D	45767190
(31640)	45958D71	4583CD20	45767190	456C888A	4583CD20	45825ED1	45825ED1	4584F455	00646C03	C34F42C0
(31680)	C3956CD9	C334759A	C01CEF1	40EE7483	405892C1	421061BA	C190071C	4591EEB5	457F0AC0	45883975
(31720)	45883975	457F0AC0	45883975	45883975	4580A1CA	4589CD5E	459AB177	459B177	45958D71	45C08C26
(31760)	45A9B177	45958D71	45A9B177	458AF455	4588C1A5	4116851E	75/28			
	FILE	44	RECORD	36	LEN	H 36 12BYTES	T 75/28			
(0)	5C3C0000	038C0000	000B7424	00204A7C	00000007	432342D4	4374E799	437A7E54	C0D224DF	408DA020
(40)	40244CD0	4142C639	428A27E	457CE335	45668B10	45668B10	457CE335	455C5FA7	454F0076	454F0076
(80)	45607123	456563EA	455C5FA7	455C5FA7	45556D46	45556D46	454F0076	455C5FA7	454985EF	4559020F
(120)	454BC5E1	00226678	C0D241AD	4024368D	43181B423	C0D2314B	408D8F94	40244575	414457C9	
(160)	422C4A70	456FB8D0	45668B10	45668B10	456FB8D0	45668B10	45668B10	45668B10	45640A81	45607123
(200)	454F0076	455C5FA7	45556D46	45556D46	455C5FA7	455C5FA7	455C5FA7	45504CF6	455448D1	00248273
(240)	00000007	4315E8C8	43680E92	43680E92	C0D230B4	408D7F06	40243E19	414613CA	422FEF46	45668B10
(280)	456FB8D0	455AEF52	45668B10	45668B10	456FB8D0	45668B10	455EB0F	45607123	454F0076	45446C85
(320)	454F0076	454985EF	454985EF	454985EF	454985EF	454985EF	454A48D1	454A48D1	00269E6F	00000007
(360)	4360ECA5	438E627E	C0D241AD	4024368D	41480940	423368F9A	456FB8D0	456FB8D0	45668B10	45668B10
(400)	4560907F	45668B10	45668B10	45668B10	45668B10	45668B10	455C5FA7	455C5FA7	45556D46	454985EF
(440)	454F0076	45556D46	454F0076	454F0076	454D4AAD	4551F898	0028BA6A	00000007	42832934	4393C917
(480)	C0D25684	408D5DE7	40242F61	414A4A7B	423729A2	456FB8D0	45668B10	45668B10	4560907F	456FB8D0
(520)	45668B10	45668B10	455C5F8F0	455C5F8F0	454F0076	454F0076	45568B10	45568B10	456FB8D0	45668B10
(560)	45556D46	454A764ED	002AD666	00000007	42143E60	43156168E5	43988B44	C0D262EA	408D4D56	
(600)	40242204	414CEF29	423AB12	45668B10	45668B10	45668B10	45668B10	45668B10	454F0076	454F0076
(640)	455B4E5	455C5FA7	455C5FA7	454F0076	454F0076	454F0076	454F0076	454F0076	454F0076	454F0076
(680)	454764ED	002CF261	00000007	C25AC527	4349190B	439CA0C8	C0D26F4E	408D3CC4	402420A7	41501F0C
(720)	423L4026	4560907F	45668B10	45668B10	456FB8D0	4560907F	456FB8D0	456FB8D0	45607123	45623984
(760)	454985EF	454F0076	45446C85	45556D46	45556D46	454F0076	454F0076	454F0076	454494DD2	002F0E5D
(800)	00000007	C2C95F72	434074B3	43A0011D	0027BAF	408D2C31	4024194A	415419D2	424182BC	45668B10